(26) Yamane, T.; Nanayama, H.; Ashida, T.; Hashimoto, K.; Sumitomo, H. *Bull. Chem. Soc. Jpn.* **1985**, *58*, 2304–2306.
(27) Ogata, N.; Tohoyama, S. *Bull. Chem. Soc. Jpn.* **1966**, *39*, 1556–1559.
(28) Ogata, N.; Asahara, T.; Tohoyama, S. *J. Polym. Sci., Polym. Chem. Ed.* **1966**, *4*, 1359–1372.
(29) Hashimoto, K.; Sumitomo, H.; Suzuki, M. *Chem. Lett.* **1986**, 767–770.
(30) Gu, Y.; Yamane, T.; Ashida, T.; Hashimoto, K.; Sumitomo, H. *Bull. Chem. Soc. Jpn.* **1986**, *59*, 2085–2088.
(31) Yamane, T.; Honda, M.; Ashida, T.; Hashimoto, K.; Sumitomo, H. submitted for publication in Bull. *Chem. Soc. Jpn.*
(32) The oligomers prepared from the racemic monomer of 1 should be racemic. In these figures only one enantiomer for each of the oligomers is shown for the simplified expression.
(33) Stowell, J. C. *Carbanions in Organic Synthesis*; Wiley: New York, 1979; p 3.
(34) Kirby, A. J. *The Anomeric Effect and Related Stereoelectronic Effects at Oxygen*; Springer-Verlag: Berlin, 1983; pp 78–134.
(35) Deslongchamps, P. *Stereoelectronic Effects in Organic Chemistry*; Pergamon: Oxford, 1983; Chapters 2, 4.

Glass Transition and Melting Behavior of Poly(thio-1,4-phenylene)

Stephen Z. D. Cheng,† Zong Quan Wu,‡ and Bernhard Wunderlich*

Department of Chemistry, Rensselaer Polytechnic Institute, Troy, New York 12180-3590.
Received April 27, 1987

ABSTRACT: Thermal properties of poly(thio-1,4-phenylene) (PPS) have been determined by differential scanning calorimetry. The solid heat capacity was measured from 220 to 350 K and the liquid heat capacity from 540 to 600 K. A detailed description of the glass transition at 363 K, its increase in heat capacity of 29.9 J/(K mol), broadness, and hysteresis effects, is reported. Three parts of the heat of fusion are identified. Their corresponding crystallinities are w^c(H), contributed by a higher melting peak; w^c(L), contributed by a lower melting peak; and w^c(C), developed on cooling after isothermal crystallization. A rigid amorphous fraction above the glass transition is needed to explain the failure of the two-phase model. Recrystallization, perfection, and reorganization of crystals are identified. The width of the melting range was found to be about 150 K. There is considerable similarity in the glass transition and melting behavior of PPS and PEEK.

Introduction

Poly(thio-1,4-phenylene) (PPS) is one of the thermoplastic polymers considered recently as a high-temperature engineering matrix material in composites. The polymer has good thermal stability and high physical strength and is easily processed.[1-4] In addition, PPS has recently generated interest as being the first melt and solution processable polymer that can be rendered electrically conductive.[5,6] From the scientific point of view, engineering processing is closely related to crystal structure, crystal morphology, crystallization kinetics, and thermal properties.

The crystal structure of PPS has been reported by Tabor et al.[7] Brady[8] has discussed in depth the effects of processing conditions on crystallinity. The growth of single crystals of PPS, as well as polycrystalline aggregates from solution,[9] the determination of morphological characteristics of melt-grown samples, including unique thin-film morphologies,[10] and the examination of structure and morphological changes accompanying doping with conductivity enhancing materials[11] have been studied widely. Crystallization kinetics of PPS, as a resin sample, has been carried out by Lovinger et al.[12] and with carbon fiber, as a matrix material, by Jog et al.[13]

Compared with those previous studies of the structure, morphology, and crystallization kinetics of PPS, the thermal properties of PPS are less well established so far. The calculation of solid heat capacity of PPS has been completed recently.[14] The glass transition temperature, T_g, of PPS varies with the measuring conditions, and lies in the range from 357 to 365 K. The absence of liquid heat capacity data of PPS made it impossible to assess the increase of heat capacity, ΔC_p, at the glass transition temperature. The equilibrium melting temperature of PPS, $T_m°$, is still uncertain. The only report of $T_m°$ for low to intermediate molecular mass PPS was between 576 and 588 K, based on $T_m - T_c$ extrapolation.[12] The heat of fusion was claimed to be 8.65 kJ/mol per repeating unit for 100% crystalline PPS.[8]

In this paper, we focus on the thermal analysis of various semicrystalline PPS samples. Both the solid and liquid heat capacities have been measured which now permits the determination of ΔC_p at T_g. The crystallinity and micromorphology dependence of ΔC_p as well as T_g are discussed. The concept of a "rigid amorphous" polymer is introduced for PPS. It is the cause of lower heat capacity of semicrystalline PPS above T_g, i.e., the rigid amorphous fraction does not contribute to the increase in heat capacity at T_g but unfreezes only at a higher temperature. Similar behavior was found, for example, for poly(aryl ether ether ketone) (PEEK).[15] The overall "rigid fraction, f_r", is computed from C_p by setting

$$f_r = 1 - [\Delta C_p(m)/\Delta C_p(a)] \qquad [\Delta C_p \text{ in J/(K mol)}] \qquad (1)$$

where ΔC_p(m) is the measured heat capacity increase at T_g for semicrystalline PPS and ΔC_p(a) applies to totally amorphous PPS. The crystallinity, in turn, is determined by

$$w^c = \Delta H_f(m)/\Delta H_f \qquad (\Delta H_f \text{ in kJ/mol}) \qquad (2)$$

where ΔH_f(m) is the measured heat of fusion of the semicrystalline sample and ΔH_f the heat of fusion of a 100% crystalline sample. If the two-phase crystallinity model is valid, f_r is equal to w^c. If not, one finds $f_r > w^c$ and a rigid amorphous fraction exists between T_g and T_m. The case of $f_r < w^c$ has not been observed.

Semicrystalline PPS shows irreversible melting. Below the main melting peak premelting peaks are found that

* Address correspondence to this author at Department of Chemistry, University of Tennessee, Knoxville, TN 37996-1600.
† Present address: Department of Polymer Science, Institute of Polymer Science, The University of Akron, Akron, OH 44325.
‡ On leave from the Chemical Fiber Research Institute, China Textile University, Shanghai, China.

0024-9297/87/2220-2802$01.50/0

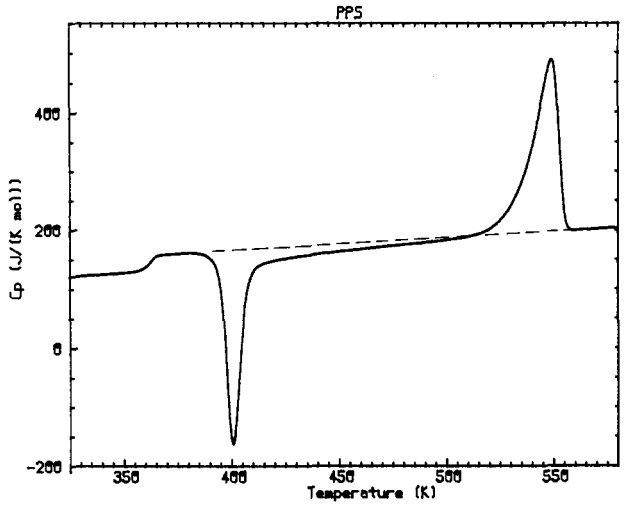

Figure 1. DSC trace of quenched PPS (liquid N_2). The glass transition temperature is at 363 K, ΔC_p at T_g is 26.3 J/(K mol), and the crystallization peak can be found at 410 K, melting occurs at about 548 K. Heating rate, 10 K/min.

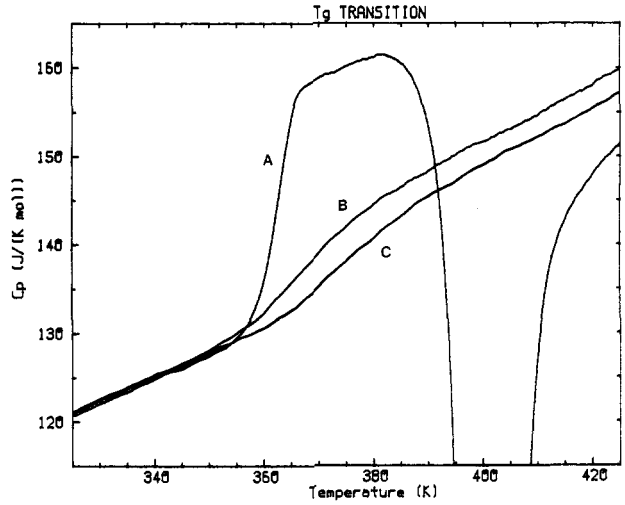

Figure 2. DSC traces of PPS in the T_g region: (A) quenched PPS sample; (B) after isothermal crystallization at 513.2 K from the melt for 0.5 h, then cooled to 315 K at 0.31 K/min; (C) on *n*-pentane induced isothermal crystallization for 0.5 h at 443.2 K from the glass and then cooled to 315 K at 0.31 K/min.[22] Heating rate 10 K/min.

are usually due to effects of defect and/or crystal reorganization, annealing, and/or premelting.[16] A study of irreversible crystal melting cannot only determine melting temperatures and crystallinity but may also provide important information on polymer crystal domain size, change of metastability, and melting kinetics.[16]

Experimental Section

Materials and Samples. The PPS for our research was acquired from Polysciences, Inc. No additional information had been provided. From our characterization, the intrinsic viscosity of the PPS is 27.655 mL/g in α-chloronaphthalene at 483.2 K. According to our unpublished results, the relationship between number-average molecular weight and intrinsic viscosity of the PPS is $[\eta]_{\alpha\text{-chloronaphthalene}}(483.2\,\text{K}) = 0.29M_n^{0.5}$. Therefore, the M_n of PPS can be estimated as 0.91×10^4.

From the thermal properties described below, the PPS sample we used is closely similar to others used for prior experiments.[8-13] Samples for differential scanning calorimetry (DSC) were prepared in aluminum pans. The sample weights were over 15 mg in order to obtain sufficiently precise heat capacity measurements, and the precision of the sample weight was within ±1 μg.

Equipment and Experiments. All samples were measured with a Perkin-Elmer DSC2 in our ATHAS Laboratory. Four temperature ranges were selected for measurements: from 220 to 340 K was the range of measurement for the solid heat capacity (below T_g), from 315 to 410 K the glass transition was analyzed, the temperature range from 375 to 580 K permits the analysis of melting, and that from 540 to 600 K is needed for the measurement of the liquid heat capacity. The DSC was calibrated in these four temperature regions individually, following the standard procedures.[17] Both temperature and heat-flow scales were corrected by using standard materials. All pan weights were kept within ± 2 μg. The repeatability of our Al_2O_3 heat capacity calibrations were within ±0.1%; the calculations were based on the data of the National Bureau of Standards.[18]

It was reported that PPS crystallized to some degree even during quenching (~5%).[3,13] We also found that the crystallization peaks are typically somewhat smaller than the melting endotherm. A DSC trace of a quenched PPS is shown in Figure 1. Figure 2 (curve A) shows a DSC heating trace comparison for PPS quenched in liquid N_2 from the melt (600 K) and two crystallized samples. Both determination of the heat capacity increase of curve A at T_g based on the solid and liquid heat capacity data of PPS (see below) and observation under a polarizing microscope[19] show a small amount of crystallinity.

Isothermal crystallization from both the melt and the glassy state were carried out. For isothermal crystallization from the melt, the samples were first heated to 600 K and held at that temperature for about 2 min to destroy all crystalline nuclei. The samples were then cooled quickly to the crystallization temperature, T_c, and kept there for the predetermined crystallization time, t_c. The isothermal crystallization was followed by cooling at a rate of 0.31 K/min to 325 K and analyzed by heating or by direct analysis from T_c without prior cooling. The analysis traces were recorded by using a 10 K/min heating rate, extending to 580 K.

For isothermal crystallization from the glassy state, the samples were heated to 600 K and held at that temperature for 2 min, as before. Then the samples were quenched in liquid N_2 directly. Different crystallization temperatures, T_c, were chosen for isothermal crystallization, and the samples were heated from below T_g to T_c at the fastest heating rate (320 K/min). The crystallization time, t_c, was counted for attainment of T_c. For analysis the same procedures (with and without cooling) were used as in the case of crystallization from the melt.

In order to study the melting behavior, different heating rates (0.31–40 K/min) were used for the analysis of samples.

Two-step isothermal crystallization experiments were performed to get information on multiple melting peaks. The first step was a crystallization at a lower T_c for time t_c; then the samples were heated to a higher T_c for completion of crystallization. The second crystallization temperature was chosen in the range of the earlier observed lower melting peaks. DSC melting traces were recorded after the samples were cooled to 325 K at 0.31 K/min.

Nonisothermal crystallization at constant cooling rates from 0.31 to 10 K/min were accomplished by cooling directly from the melt after being kept at 600 K for about 2 min.

The glass transition region is characterized by five temperatures, as was illustrated before:[15] T_b, the first perceptible beginning of the glass transition; T_1 and T_2, the extrapolated beginning and end of the glass transition (indicative of the broadness of the major portion of the glass transition); T_g, the glass transition temperature (chosen at half-devitrification when judged by the heat capacity increase); and finally, T_e, the end of the glass transition, which is reached when the heat capacity of the amorphous portion reaches the liquid heat capacity.

To study the hysteresis at the glass transition, the samples were heated to just above T_g (370 K) and cooled at various chosen rates before analysis. The hysteresis peak temperature was recorded. The endothermic peak area above base line of the heat capacity above T_e was measured for the discussion of hysteresis.

Results

Solid State Heat Capacities of PPS. The experimental temperature range for heat capacity measurements was 230–330 K. Both amorphous and semicrystalline PPS heat capacities agree to be better than ±1% in this temperature range. A tendency of lower heat capacities for semicrystalline PPS can be suggested but is well within

Table I
Thermal Properties of PPS in the Glass Transition Region Measured on Heating at 10 K/min

cooling rate	T_b, K	T_1, K	T_g, K	T_2, K	T_e, K	ΔT_1, K[a]	ΔT_2, K[b]	ΔC_p, J/(K mol)
A. Nonisothermal Crystallization on Cooling from the Melt to below T_g								
quenched	352	358	363	366	372	8	20	26.3
cooling −0.31 K/min	352	359	368	377	390	18	38	9.0
cooling −2.5 K/min	352	359	368	378	392	19	40	8.6
cooling −10 K/min	352	359	369	380	395	21	43	8.3
B. Isothermal Crystallization from the Glass, Followed by Cooling at −0.31 K/min to below T_g								
443.2 K, 0.5 h	352	363	378	388	402	25	50	9.2
463.2 K, 0.5 h	352	363	376	387	400	24	48	9.5
483.2 K, 0.5 h	352	363	373	386	398	23	46	10.0
C. Isothermal Crystallization from the Melt, Followed by Cooling at −0.31 K/min to below T_g								
503.2 K, 0.5 h	352	357	370	384	395	27	43	9.2
513.2 K, 0.5 h	352	356	369	381	393	25	41	9.2
523.2 K, 1 h	352	356	368	381	391	25	39	9.2
533.2 K, 3 h	352	356	367	378	388	22	36	9.3
543.2 K, 24 h	352	356	365	375	386	19	34	9.2

[a] $\Delta T_1 = T_2 - T_1$. [b] $\Delta T_2 = T_e - T_b$.

experimental error. A calculation of heat capacities of fully amorphous PPS below T_g had been performed earlier by using independently evaluated group vibration spectra and the Tarasov temperatures $\theta_1 = 566.3$ K and $\theta_3 = 40$ K for the skeletal vibrations (five modes of vibration).[14] The heat capacities measured in this research were fitted to the following equation (root mean square deviation, ±0.2%)

$$C_p = \exp[0.109038(\ln T)^3 - 1.7846(\ln T)^2 + 10.7735(\ln T) - 18.9156] \quad (3)$$

in J/(K mol) with 15 runs on 10 samples in the temperature range 220–340 K with ±1.5% agreement of the various runs at any one temperature. Equation 3 fits the calculated heat capacities to +0.2 ± 0.2%, well within the experimental error.

Liquid Heat Capacities and Glass Transition of Amorphous PPS. In the temperature range between 540 and 600 K, liquid heat capacities of PPS have been measured. The measurements could begin at 540 K since one can cool PPS sample from the melt without crystallization. The supercooling needed for molecular nucleation[20] leads to a metastable melt of which the crystal does not grow in the measuring time period. A linear relationship between heat capacities and temperature was found, as usual, and was expressed as

$$C_p = 0.12574T + 119.73 \quad (4)$$

in J/(K mol). Detailed thermodynamic functions will be reported elsewhere.[21] The extrapolation of eq 4 to the glass transition region provides, when combined with the calculated solid heat capacity of PPS, the heat capacity increase at T_g. The calculation of ΔC_p at 363 K is 29.9 J/(K mol). Figure 2 shows the experimental data of ΔC_p of quenched PPS (curve A) with a ΔC_p of 26.3 J/(K mol). It indicates that there is about 11% rigid fraction (f_r) formed during quench.

Glass Transitions of Semicrystalline PPS. In Table I, data for 12 samples of different thermal history are listed. Both the broadness of the major glass transition region ($\Delta T_1 = T_2 - T_1$) and the width of the glass transition ($\Delta T_2 = T_e - T_b$) increase with cooling rate for nonisothermal crystallization and decrease with increasing crystallization temperature, T_c, for isothermal crystallization. Since the beginning of the glass transition temperature, T_b, is not changed for any of the samples, the decrease in ΔT_2 is due to a shift of the end of glass transition to lower temperatures with increasing T_c or decreasing cooling rate. The change of the glass transition temperature as a function of crystallization temperature is shown in Figure 3. Figure 2, above, shows three limiting DSC curves for the glass transition region of PPS.

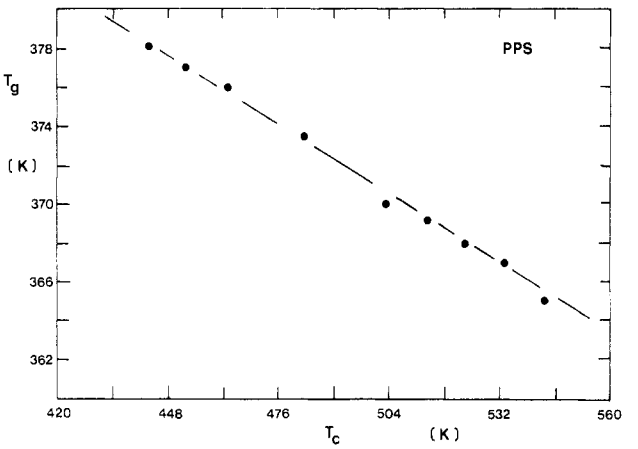

Figure 3. Relationship between glass transition temperature T_g and isothermal crystallization temperature T_c.

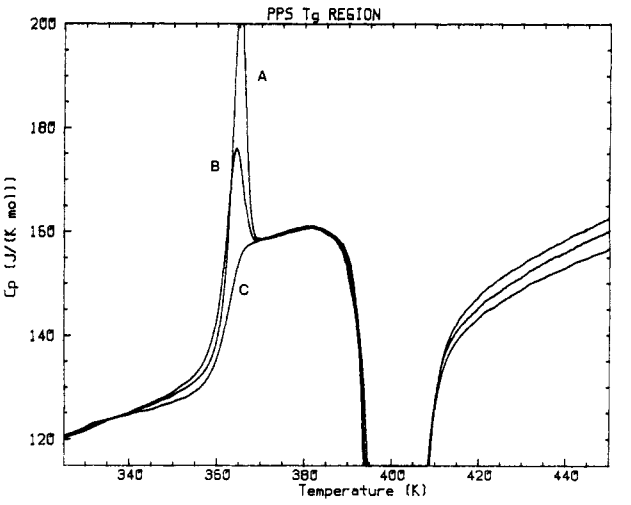

Figure 4. Hysteresis of quenched PPS samples cooled at different cooling rates through T_g from 370 K: (A) 0.31 K/min; (B) 2.5 K/min; (C) quenched to liquid N_2; heating rate 10 K/min.

Hysteresis in the T_g Region. Figure 4 shows the hysteresis of the heat capacity of quenched PPS in the glass transition region. The largest endothermic hysteresis peak is observed for the cooling rate 0.31 K/min (ΔH = 122 J/mol). With increasing cooling rate, the endotherm decreases, as shown in Figure 5. The hysteresis peak disappears totally when the heating rate is equal to the

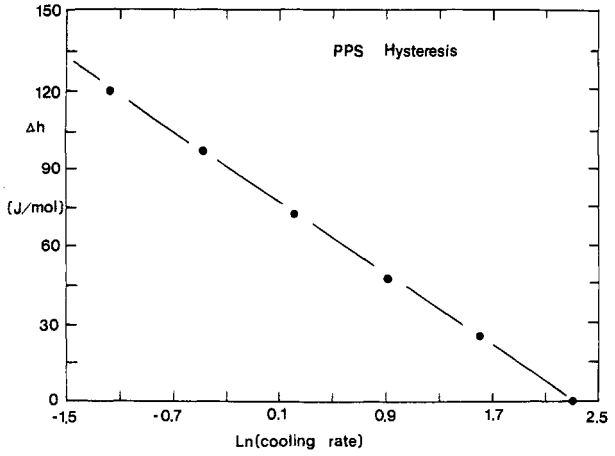

Figure 5. Relationship between the enthalpy of the hysteresis peak and the logarithm of cooling rate for liquid-N_2-quenched PPS samples. Heating rate is 10 K/min.

prior cooling rate. Finally, the quenched PPS sample shows a small, but noticeable, exothermic hysteresis just below T_g. Such exothermic hysteresis becomes more obvious on faster quenching of PPS samples (in *n*-pentane externally cooled by liquid N_2).

There is no hysteresis effect for the semicrystalline PPS, even though prior cooling rates of 0.31 K/min were used (see curves B and C in Figure 2).

The influence of slow cooling through the glass transition on crystallization can be observed by comparing the exotherms in Figure 4. Slightly broader crystallization peaks are seen when the slowest cooling rate (0.31 K/min) is used (about 1 K on the low-temperature side of the crystalline peak, the high-temperature crystallization changes little). The heat capacities after crystallization are different up to the major melting. The slower the prior cooling rate, the lower the heat capacities. Quantitatively, the difference in C_p after quench or slow cooling through T_g is 6–9 J/(K mol). Such a change in heat capacity must be linked to changes in the rigid amorphous fraction since little difference exists in the heats of fusion. A change in heat capacity of 6–9 J/(K mol) corresponds to 20–30% rigid fraction.

Heat Capacity of Semicrystalline PPS above T_g. As described above, both solid and liquid heat capacity data are available. This permits the determination of the rigid fraction at the glass transition temperature, T_g, and its change up to the melting transition temperature, T_m. Figure 6 shows the rigid fraction dependence of the heat capacity in this temperature range for both isothermal and nonisothermal crystallization. Up to 410 K, the semicrystalline PPS heat capacity data fit the calculation. Above this an increasingly positive deviation occurs. This deviation increases with decreasing rigid fraction and merges at higher temperatures into the lower temperature melting peaks (see below).

Isothermally crystallized samples at T_c = 503.2 K, i.e., crystallized from the glass, show a heat capacity after the lower melting peak that is below that expected for the given rigid fraction. For example, PPS crystallized at T_c = 443.2 K has a rigid fraction of 26% based on the ΔC_p at T_g, but its heat capacity at 470 K would correspond to a f_r = 77%. This is far outside any possible error and must be an indication of latent heat effects due to recrystallization or reorganization (see below). With increasing T_c, this negative deviation in the heat capacity decreases, but a small amount remains for all samples crystallized from the glass. On crystallization from the melt, the two melting peaks overlap. The heat capacity increases continuously

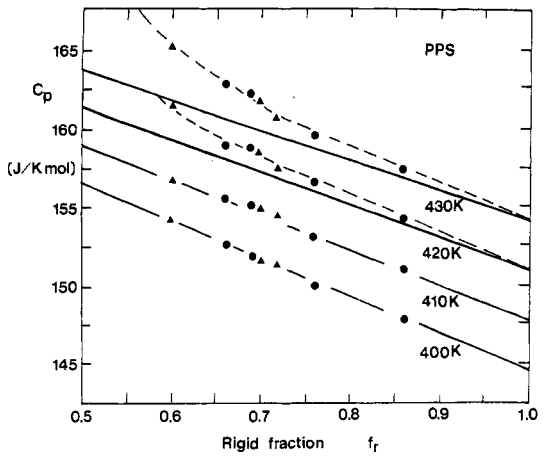

Figure 6. Rigid amorphous fraction dependence of heat capacity above T_g. The solid lines are calculated on the basis of eq 3 and 4. Circles are for isothermal crystallization data; triangles are for nonisothermal crystallization data. (Special samples: f_r = 0.60, the PPS sample was cooled at 80 K/min to 315 K; f_r = 0.76 and 0.86, the PPS samples were quenched in an *n*-pentane cooling bath and, then, isothermally crystallized at 443.2 and 483.2 K, respectively. See ref 22. All other samples are listed in Table II).

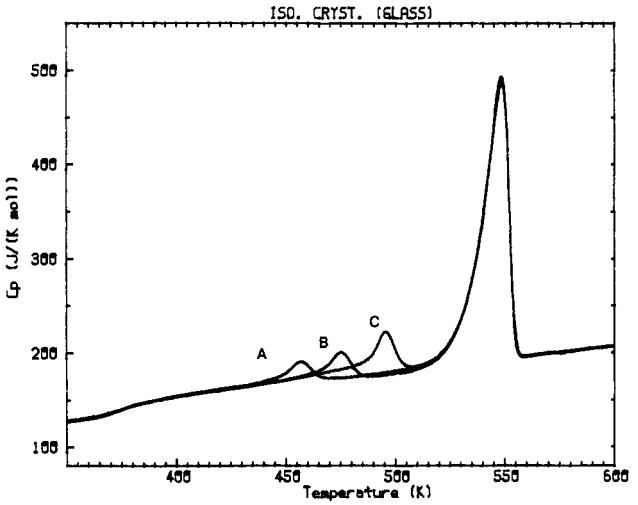

Figure 7. DSC melting traces after isothermal crystallization of PPS from the glass at 443.2, 463.2, and 483.2 K for 0.5 h (curves A to C, respectively).

beyond that calculated in Figure 6 from about 420 K to the beginning of melting at about 525 K. The determination of the latent heat of fusion must thus be started at 420 K for all samples and extended to the liquid state at about 570 K; i.e., the melting range is about 150 K wide.

The Melting Temperature of PPS. For isothermal crystallization from the melt and the glass, at different T_c, all DSC melting traces are characterized by two melting peaks. The smaller, low-temperature melting peak can be observed about 10–20 K above the crystallization temperature, and the larger melting occurs above 548 K. Figures 7 and 8 show the DSC traces. At T_c = 483.2 and 503.2 K the crystals grow so fast that isothermal conditions are reached only after crystallization begins. It is clear that the lower melting peak temperatures depend strongly on crystallization conditions. The higher melting peak temperatures, however, are almost constant below T_c = 503.2 K and increase at higher temperature. The relationship between T_m and T_c for both melting peaks is shown in Figure 9. An extrapolation of this relationship to T_c = T_m leads to temperatures in the range 620–630 K.

For nonisothermal crystallization two melting peaks are still recognizable and are shown in Figure 10. Both

Table II
Thermal Properties of PPS in the Melting Transition Region Measured on Heating at 10 K/min

T_c, K, or cooling rate	W^c(T)	W^c(H)	W^c(L)	W^c(I)	W^c(C)	f_r	$f_r - W^c$(T)
A. Isothermal Crystallization from the Glass, then Cooling at −0.31 K/min							
443.2 K, 0.5 h	0.43	0.40	0.02	0.42	0.01	0.69	0.26
463.2 K, 0.5 h	0.445	0.40	0.03	0.43	0.015	0.68	0.24
483.2 K, 0.5 h	0.46	0.40	0.04	0.44	0.02	0.67	0.21
B. Isothermal Crystallization from the Melt, then Cooling at −0.31 K/min							
503.2 K, 0.5 h	0.52	0.41	0.05	0.46	0.06	0.69	0.17
513.2 K, 0.5 h	0.53	0.39	0.07	0.46	0.07	0.69	0.16
523.2 K, 1 h	0.55	0.34	0.12	0.46	0.09	0.69	0.14
533.2 K, 3 h	0.57	0.29	0.17	0.46	0.11	0.69	0.12
543.2 K, 24 h	0.59	0.23	0.22	0.45	0.14	0.69	0.10
C. Nonisothermal Crystallization from the Melt							
10 K/min	0.46	0.35	0.11			0.72	0.26
2.5 K/min	0.48	0.34	0.14			0.71	0.23
0.31 K/min	0.52	0.35	0.17			0.70	0.18

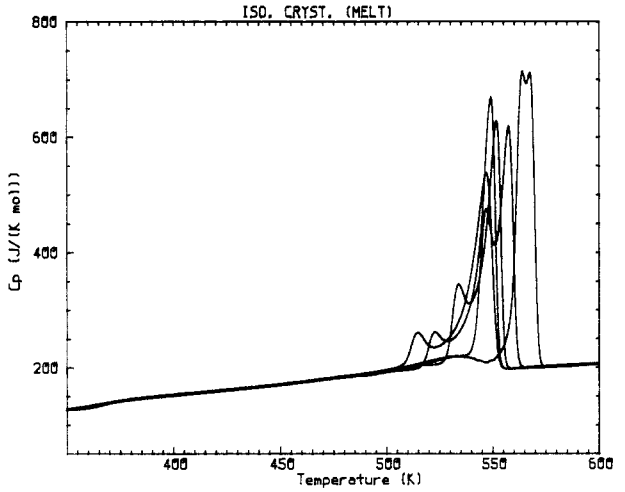

Figure 8. DSC melting traces of isothermal crystallization of PPS from the melt at 503.2, 513.2, 523.2, 533.2, and 534.2 K for 0.5 h for the first two samples, and then for 1, 3, and 24 h for the latter 3 (curves from left to right, respectively).

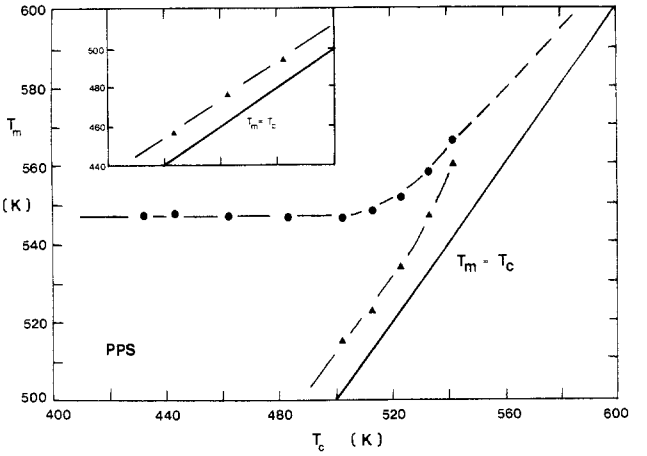

Figure 9. Relationship between crystallization temperature T_c and melting temperature T_m of PPS. The circles are melting temperatures of the high-melting peak and the triangles are those of the low-melting peak crystallized at different temperature. The solid line is for $T_m = T_c$.

melting peak temperatures decrease with increasing cooling rates. Again, the heat capacities start deviating from a fixed rigid fraction at about 420 K (see Figure 6).

The Heat of Fusion of PPS. The determination of solid and liquid heat capacities of PPS permits also a quantitative study of the heats of fusion by providing reliable base lines. From the isothermal crystallization experiments, three parts of the heat of fusion can be identified: the heat of fusion connected with the of fusion of the higher temperature melting peak, that of the lower temperature melting peak, and the contribution from the crystals grown during cooling at 0.31 K/min. The last portion was determined by comparison of samples analyzed with and without cooling prior to heating. For nonisothermal crystallization only the first two parts of the heat of fusion can be evaluated. The results are listed in Table II in which w^c(T) is the total crystallinity of the samples; w^c(H) is the crystallinity of the higher temperature melting peak, w^c(L) is the crystallinity of the lower temperature melting peak, and w^c(C) is a crystallinity contributed during cooling; finally w^c(I) = w^c(H) + w^c(L).

For isothermal crystallization from the glassy state w^c(T) and w^c(L), as well as w^c(C), increase with increasing T_c. The value of w^c(H), however, stays almost constant. The values of w^c(T), w^c(L), and w^c(C) increase also in the case of isothermal crystallization from the melt, but w^c(H) decreases. A compensation between w^c(H) and w^c(L) leads to an almost constant w^c(I) (about 0.46). The same results for w^c(H) and w^c(L) can be observed from the isothermal

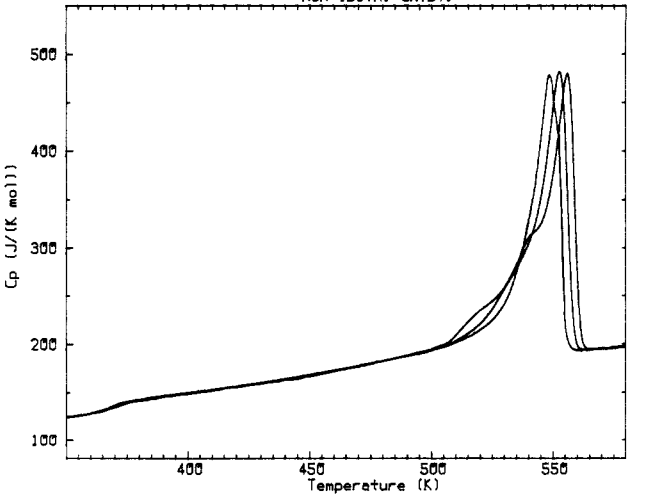

Figure 10. DSC melting traces after nonisothermal crystallization at different cooling rates (0.31, 2.5, and 10 K/min, higher melting peaks from right to left, respectively).

crystallization experiments without cooling before analysis. The total crystallinity of the isothermally melt crystallized PPS increases thus only with T_c due to larger crystallization on cooling.

In Table II, the rigid amorphous fractions [$f_r - w^c$(T)] are also listed, based on the comparison between ΔC_p at T_g (eq 1) and the total crystallinity (eq 2). One can find that the rigid fraction decreases with increasing T_c for

Table III
Melting Behavior at Different Heating Rates at the Given Crystallization Temperatures

heating rates, K/min	W^c(L)	W^c(H)	W^c(I)
	T_c = 463.2 K, t_c = 0.5 h		
2.5	0.01	0.42	0.43
10	0.03	0.40	0.43
20	0.04	0.39	0.43
40	0.05	0.38	0.43
	T_c = 503.2 K, t_c = 0.5 h		
0.31	0.01	0.45	0.46
2.5	0.035	0.425	0.46
10	0.05	0.41	0.46
20	0.06	0.40	0.46
40	0.07	0.38	0.45
	T_c = 533.2 K, t_c = 3 h		
0.31	0.07	0.39	0.46
2.5	0.13	0.33	0.46
10	0.17	0.29	0.46
20	0.19	0.27	0.46
40	0.21	0.24	0.45

isothermal crystallization (both from the glass and from the melt) from 26% at T_c = 443.2 K to 10% at T_c = 543.2 K.

For nonisothermal crystallization w^c(T) increases with decreasing cooling rate and so does the lower melting peak crystallinity, w^c(L). The higher melting peak crystallinity, w^c(H), however, does not change as also shown in Figure 10. The rigid amorphous fraction of the amorphous portion decreases from 48% at a cooling rate of 10 K/min to 38% at 0.31 K/min, as shown in Figure 11.

Conversion between the Two Melting Peaks. Different heating rates have been used for analysis after isothermal crystallization without cooling. The crystallinity of the lower melting peak decreases with heating rate and the crystallinity of the higher melting peak increases, keeping w^c(I) constant. The results are listed in Table III, and Figure 12 shows a plot of crystallinity, w^c(L), vs. the logarithm of the heating rate. The conversion rates between the two melting peaks (the slopes of the linear relationship between w^c(L) and ln q, dw^c(L)/d ln q) are 0.012, 0.015, and 0.029 at T_c = 463.2, 503.2, and 533.2 K, respectively, where q is the heating rate in K/min.

Melting after Two-Step Isothermal Crystallization. Figure 13 shows a DSC trace for the two-step isothermal crystallization at T_c = 513.2 K, followed by T_c = 533.2 K. Melting traces after one-step isothermal crystallization at 513.2 and 533.2 K are included for comparison. As has been found for PEEK,[15] the lower melting peak temperature corresponds to that of the one-step crystallization at the higher of the two steps. The higher melting peak temperature, in contrast, is always that fixed at the first step of crystallization, i.e., there is a "memory effect".

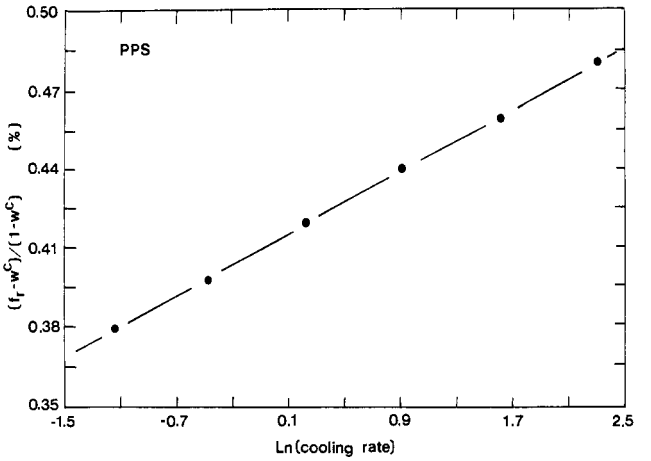

Figure 11. Relationship between $(f_r - w^c)/(1 - w^c)$ and the logarithm of cooling rate.

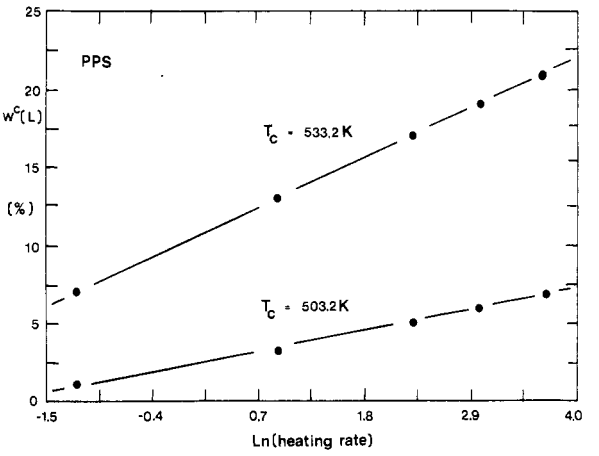

Figure 12. Relationship between the lower melting peak crystallinity, w^c(L), and the logarithm of the heating rate.

Table IV lists the detailed analyses for three two-step isothermal crystallizations as well as the corresponding one-step crystallizations. One can find that w^c(L) and w^c(H) in a two-step crystallization are changed from the one-step values, but w^c(T) and w^c(I) do not vary. For

Table IV
Comparison of Thermal Properties Obtained by One-Step and Two-Step Isothermal Crystallization

T_c/K, t_c/h[a]	T_g/K	T_m(L)/K	T_m(H)/K	W^c(T)	W^c(L)	W^c(H)	$f_r - W^c$(T)
			A				
483.2, 0.5	373	495	548	0.46	0.40	0.40	0.21
503.2, 0.5	370	515	548	0.52	0.05	0.41	0.17
483.2, 0.5							
503.2, 0.5	370	515	548	0.52	0.06	0.40	0.17
			B				
503.2, 0.5	370	515	548	0.52	0.05	0.41	0.17
523.2, 1	368	534	552	0.55	0.12	0.34	0.14
503.2, 0.5							
523.2, 1	368	534	548	0.55	0.14	0.32	0.14
			C				
513.2, 0.5	369	523	549	0.53	0.07	0.39	0.16
533.2, 3	367	547	558	0.57	0.17	0.29	0.12
513.2, 0.5							
533.2, 3	367	(547)	549	0.57	*b*	*b*	0.12

[a] Single temperatures and times express one-step isothermal crystallization experiments; double temperatures and times express two-step isothermal crystallization experiments. [b] Two peaks overlapped; W^c(L) and W^c(H) cannot be distinguished.

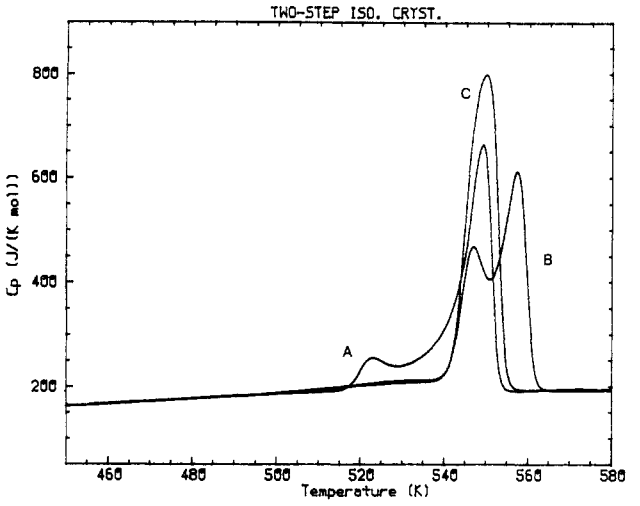

Figure 13. Two-step isothermal crystallization from the melt. (A) T_c = 513.2 K, 0.5 h, cooled to 315 K at 0.31 K/min before recording; (B) T_c = 533.2 K, 3 h, cooled to 315 K at 0.31 K/min before recording; (C) T_c = 513.2 K, 0.5 h, heated to 533.2 K at 10 K/min, another 3-h crystallization followed by cooling to 315 K at 0.31 K/min before recording at 10 K/min.

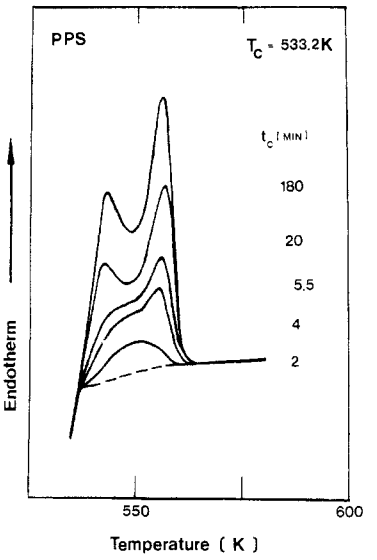

Figure 14. Analysis of crystals grown at 533.2 K at different lengths of time. Dashed line estimated base line.

example, w^c(L) of the two-step crystallization in the B set is 14%, 2% higher than for the one-step isothermal crystallization at T_c = 523.2 K and 9% higher than for the one-step isothermal crystallization at T_c = 503.2 K. The higher melting peak area is 32%, 2%, and 9% lower than for one-step isothermal crystallization at T_c = 523.2 and 503.2 K, respectively. In the C set of Table IV, one can see that the higher melting peak of the first-step isothermal crystallization overlaps with lower melting peak of the second step. Only one melting peak can be observed. Even though the higher melting peak of the one-step isothermal crystallization at T_c = 533.2 K is 9 K higher than that at T_c = 513.2 K (see also Figure 8).

Sequence of Crystallization. To understand the sequence of crystallization of PPS, isothermal crystallizations at 533.2 K were performed by interrupting crystallization at different times. Without cooling, the immediate analyses are shown in Figure 14. After 2 min, there is only a broad melting peak, intermediate between the high- and low-temperature melting peaks. At later times the melting peak gets sharper, and the higher melting peak develops. With increasing time a distinct lower melting peak can be seen after about 5 min. The ratio of w^c(L) to w^c(H) increases with time and both peaks move to slightly higher melting temperature as crystallization proceeds.

Discussion

Heat Capacities. As expected, the low-temperature heat capacities (230–330 K, eq 3) are practically independent of the rigid fraction and the calculated heat capacities using an approximate vibrational frequency spectrum[14] agree well with the large number of new measurements of this research.

The liquid heat capacity given by eq 4 can be compared to the liquid heat capacity of other phenylene-containing polymers.[23] Subtracting the contribution of the phenylene group, a heat capacity contribution with negative temperature coefficient (−0.0208T) results for the sulfur group, as expected from similar contributions of oxygen (−0.00711T).[24]

Rigid Amorphous PPS. The failure of the two-phase model in some polymers was recognized for a long time. Nevertheless, a quantitative study of this phenomena via thermal analysis was possible only very recently, starting with poly(oxymethylene).[25,26] It has also been proven that the rigid amorphous fraction depends on the different crystallization conditions for PEEK[15] and, now, also for PPS. In fact, the rigid amorphous fraction permits the quantitative characterization of a linkage between crystalline and amorphous phases. We suggest that the micromorphological effect giving rise to the rigid amorphous fraction must be of a nanometer scale to be detected at the glass transition. For a long time arguments existed for the description of the nonequilibrium, semicrystalline macromolecules.[27] Two models have been suggested: one based on folding by adjacent reentry folds and the other based on fringed micelles. In reality, the structure should be thought of being in between both models.[28] The quantitative evaluation of the rigid amorphous fraction may be a first step to assess interfacial strain.

With decreasing crystallization temperature, one assumes crystals to become less perfect. The longitudinal and lateral sizes of the crystals usually decrease. It seems thus reasonable that the interface regularity decreases also. Loose folds, cilia, and ties should increase. Furthermore, an increased crystal growth rate leads to a decrease of time for the crystals to adjust into the locally energetically most favorable states. Internal stress cannot be released during crystal growth and concentrates at the boundary between crystalline and amorphous phases. Therefore, the necessary condition for the existence of a rigid amorphous phase is the formation of loose folds, cilia, and ties, i.e., molecules that cross the crystalline–amorphous phase boundary and the sufficient condition that there is, in addition, internal stress. The rigid amorphous fraction must depend on the area of phase boundary, the degree of irregularity, and the molecular mobility.

The high-melting polymers containing phenylene groups are expected to have a higher tendency to have rigid amorphous portions because of their chain stiffness. The study of the change in rigid amorphous material with temperature for these polymers is complicated by the early melting of the poor crystals (see below) with high rigid amorphous fractions. Nevertheless, one can find that at least over the 20–30 K above T_c there is no indication of a change in rigid amorphous fraction for both PPS and PEEK.[15] A possible "glass transition of the rigid amorphous fraction" above 420 K for PPS would merge with the lower temperatures of fusion and thus be undetectable.

Glass Transition Region. Table I and Figures 1 and 2 show that the quenched PPS has the sharpest and largest

glass transition. The observed ΔC_p = 26.3 J/(K mol) is, however, 11% lower than the increase in heat capacity at T_g based on the calculated solid and liquid heat capacities. This is an indication of some crystallinity and a rigid amorphous fraction even on such fast quenching. Any additional crystallization broadens the glass transition range and shifts its end, T_e, to higher temperatures by as much as 36 K. The glass transition temperature, T_g, itself is shifted by as much as 15 K (all at 10 K/min heating rate). The more restrictive the crystallization (i.e., the faster the cooling rate or the lower the crystallization temperature), the larger is the effect. Figure 3 shows the change of T_g as a function of crystallization temperature. Coupled with this broadening of the glass transition range is an increase of the rigid amorphous PPS above T_g (Table II). For the crystallization at 443.2 K it reaches 46% of the remaining amorphous fraction (0.57). It indicates that, indeed, the existence of rigid amorphous PPS hinders also molecular motion at T_g and leads to a broader distribution of relaxation times.

The hysteresis behavior of almost amorphous PPS appears similar to that of other polymers analyzed (see Figure 4).[29,30] Different from the observation of PEEK,[15] however, is that Δh of the hysteresis of PPS is smaller than that of PEEK cooled at the same rate through T_g.[15] This may be due to the remaining rigid fraction even in quenched PPS. The somewhat earlier crystallization of PPS slowly cooled through T_g and the larger rigid amorphous fraction are also more in line with reorganization of a small amount of crystals than better relaxed amorphous samples. Hysteresis of higher crystallinity PPS (above 0.40 in this paper) cannot be observed under our measuring conditions. The broadening of the glass transition region alone (see Table I) is not sufficient to explain the disappearance of hysteresis. The crystalline–amorphous interface must change the time dependence of the glass transition, as was found recently for other high-melting-temperature polymers containing phenylene groups, e.g., poly(ethylene terephthalate).[31]

The small exotherm at 350–360 K of the fast-quenched sample is less than on theoretical grounds, as in the polystyrene case.[29]

Irreversible Crystal Melting. Before the discussion of melting of PPS, one needs to review the information on equilibrium melting. The equilibrium melting temperature of PPS is not well established. The observed melting at 558 K refers obviously to irreversible crystal melting. The method of extrapolation of T_m as a function of T_c seems not reliable enough since it is difficult to grow polymer crystals at low supercooling.[28] The extrapolated data of Lovinger et al.[12] (576–588 K) and from us (620–630 K) are examples for the degree of uncertainty of this method.

A better extrapolation would be that of T_m versus crystal size. Since it is unlikely that most crystals of high melting temperature polymers are laterally large lamellae, the usual equation relating T_m to the reciprocal of lamellar thickness may have to be expanded to include lateral crystal dimensions. Based on lamellar thickness only an equilibrium melting temperature of 593 K was extrapolated.[32]

The heat of fusion was determined by Brady,[8] who measured a ΔH_f of 5.43 kJ/mol for a PPS sample of 63% crystallinity as determined by X-ray diffraction. This gives a value of 8.65 kJ/mol per repeating unit for the heat of fusion of 100% crystalline PPS. No further information has been provided so far. These values lead to a first entropy of fusion estimate of 13.8 J/(K mol) per repeating unit, a reasonable value.[16]

Turning to nonequilibrium one may find broadening and lowering of melting peaks due to small crystal size and defects, change of stability of crystals during heating for analysis due to annealing, or recrystallization after initial melting and possibly superheating.[16]

The melting temperatures of Figure 9 shows typical polymer behavior.[16] The low-temperature melting peak is similar to the often observed "annealing peaks".[16] The higher melting peak stays constant for crystallization temperatures below 503.2 K because of reorganization. Above T_c of 503.2 K, the crystals do not perfect on heating and the higher T_m and narrower melting peak are an indication of more perfect crystals grown at T_c.

Three different crystallinities have been distinguished (Table II and Figures 7, 8, and 10). According to Figure 14 some high-melting crystals develop first, followed by the lower melting crystals. The high-melting portion seems to grow out of an intermediate melting fraction, similar to prior observations on polyethylene[33] and PEEK.[15] Two additional facts are of importance: (1) An increase in heating rate for analysis increases the ratio between lower to higher melting crystals and (2) there is an exothermic contribution to the heat capacity of samples crystallized below T_c = 503.2 K. The first indicates rearrangement, the second, recrystallization. Recrystallization seems to be the major contribution for crystals grown at lower temperatures. Reorganization seems dominant for crystals grown at higher temperatures.

From the two-step isothermal crystallization (see Figure 13 and Table IV) recrystallization and reorganization can be distinguished. The higher melting crystallinity, w^c(H), of the two-step crystallization is for set B 9% lower than in one-step isothermal crystallization at the higher temperature. No further annealing occurs for the initially grown high-melting crystals. The lower melting crystals grown during the first isothermal crystallization must melt on heating to the second crystallization step. Recrystallization occurs and leads to the new low-temperature melting peak, governed by the higher T_c of the second step. Reorganization, in contrast, must occur during heating of the one-step grown crystals because the ratio of low- to high-melting crystals changes with heating rate (Figure 12). This reorganization process becomes much slower for the two-step isothermal crystallization on heating, i.e., the perfection of the lower melting crystals on heating is hindered by the already present higher melting peak. Furthermore, most of the rigid amorphous fraction (and shift in T_g) is caused by the lower melting peak crystallinity, w^c(L), and its true influence on the overall polymer is thus much larger than indicated by w^c(L).

Finally, the additional crystallinity contributed on cooling after completion of crystal growth at T_c, w^c(C), increases continuously with T_c and accounts for the major change in w^c(T) with T_c. The crystals grown on cooling are of lower perfection. There is also a close relationship between the crystals grown on cooling and the rigid amorphous fraction. When fewer of these crystals are formed, the rigid amorphous fraction is higher (see also Table II).

Conclusions

With the well-established heat capacities of solid and liquid PPS, it is possible to gain a more detailed description of the semicrystalline polymer. The phase transition is shown to broaden to higher temperature on partial crystallization. A rigid amorphous fraction can be identified and has been studied as a function of crystal perfection. As with other polymers, the hysteresis is reduced on partial crystallization. Annealing, recrystallization, and

crystal perfection have been identified. During crystallization the high-melting crystals grow first and seem to reorganize from an intermediate crystal population. The low-melting crystals grow later. On heating for analysis the low- to high-melting ratio changes due to annealing.

Acknowledgment. The research was supported by the National Science Foundation, Polymer Program, Grant DMR 83-17097.

Registry No. PPS, 25212-74-2.

References and Notes

(1) Hartness, J. T. *Natl. SAMPE Symp. Exhib.* [*Proc.*] **1980**, *25*, 376.
(2) Brady, D. G. *J. Appl. Polym. Sci., Appl. Polym. Symp.* **1981**, *36*, 231.
(3) Martin, C. C.; O'Connor, J. E.; Lou, A. Y. *SAMPE Q.* **1984**, July 12.
(4) Hill, H. W.; Brady, D. G. *Polymers Containing Sulfur–Polyphenylene Sulfide*; Encyclopedia of Chemical Technology, 1982; Vol. 18, p 793.
(5) Frommer, J. E.; Elsenbaumer, R. L.; Eckhardt, H.; Chance, R. R. *J. Polym. Sci., Polym. Lett. Ed.* **1983**, *21*, 39.
(6) Clarke, T. C.; Kanazawa, K. K.; Lee, V. Y.; Rabolt, J. F.; Reynolds, J. R.; Street, G. B. *J. Polym. Sci., Polym. Phys. Ed.* **1982**, *20*, 117.
(7) Tabor, B. J.; Magre, E. P.; Boon, J. *Eur. Polym. J.* **1971**, *7*, 1127.
(8) Brady, D. G. *J. Appl. Polym. Sci.* **1976**, *20*, 2541.
(9) Padden, F. J., Jr.; Lovinger, A. J.; Davis, D. D., manuscript in preparation.
(10) Lovinger, A. J.; Padden, F. J., Jr.; Davids, D. D. *Macromolecules*, in press.
(11) Lovinger, A. J.; Davids, D. D., unpublished results.
(12) Lovinger, A. J.; Davis, D. D.; Padden, F. J., Jr. *Polymer* **1985**, *26*, 1595.
(13) Jog, J. P.; Nadkarni, V. M. *J. Appl. Polym. Sci.* **1985**, *30*, 997.
(14) Cheng, S. Z. D.; Lim, S.; Judovits, L.; Wunderlich, B. *Polymer* **1987**, *28*, 10.
(15) Cheng, S. Z. D.; Cao, M.-Y.; Wunderlich, B. *Macromolecules* **1986**, *19*, 1868.
(16) Wunderlich, B. *Macromolecular Physics*; Academic: New York, 1980; Vol. 3.
(17) Wunderlich, B.; Bopp, R. C. *J. Thermal Anal.* **1974**, *6*, 335. See also: Mehta, A.; Bopp, R. C.; Gaur, U.; Wunderlich, B. *J. Thermal Anal.* **1978**, *13*, 197.
(18) Ginnings, D. C.; Furukawa, G. T. *J. Am. Chem. Soc.* **1953**, *75*, 522.
(19) The PPS sample was heated to 590 K and then quenched with liquid N_2. There are some small birefringent spots at room temperature. Estimates of the crystallinity for the quenched samples are less than 7%.
(20) Cheng, S. Z. D.; Wunderlich, B. *J. Polym. Sci., Polym. Phys. Ed.* **1986**, *24*, 577, 595.
(21) Cheng, S. Z. D.; Wunderlich, B., manuscript in preparation.
(22) Unpublished data from our laboratory. The PPS samples were quenched in *n*-pentene cooled by liquid N_2. It yielded quick cooling but induces crystallization due to the solvent (*n*-pentane) to higher crystallinities. Isothermal crystallization of those quenched PPS samples from the glassy state shows no lower melting peak during subsequent heating.
(23) Cheng, S. Z. D.; Wunderlich, B. *J. Polym. Sci., Polymer Phys. Ed.* **1986**, *24*, 1755.
(24) Suzuki, H.; Wunderlich, B. *J. Polym. Sci., Polymer Phys. Ed.* **1985**, *23*, 1671.
(25) Suzuki, H.; Wunderlich, B. *Makromol. Chem.* **1985**, *189*, 1109.
(26) Suzuki, H.; Wunderlich, B. *Br. Polym. J.* **1985**, *17*, 1.
(27) For a recent review, see, for example: *Faraday Discuss. Chem. Soc.* **1968**, 68.
(28) Wunderlich, B. *Macromolecular Physics*; Academic: New York, 1973; Vol. 1.
(29) Wunderlich, B.; Bodily, D. M.; Kaplan, M. H. *J. Appl. Phys.* **1964**, *35*, 95.
(30) Wolpert, S. M.; Weitz, A.; Wunderlich, B. *J. Polym. Sci., Polym. Phys. Ed.* **1971**, *9*, 1887.
(31) Menczel, J.; Wunderlich, B. *J. Polym. Sci., Polym. Lett. Ed.* **1981**, *19*, 261.
(32) Wu, Z. Q.; Zhang, A. Q.; Cheng, S. Z. D.; Wunderlich, B., manuscript in preparation.
(33) Wunderlich, B.; Melillo, L.; Cormier, C. M.; Davidson, T.; Snyder, G. J. *Macromol. Sci. Phys.* **1967**, *B1*, 485.

Structure and Crystallization of n-$C_{21}H_{44}$, n-$C_{36}H_{74}$, and Low Molecular Weight Polyethylene Glasses

H. Hagemann,† H. L. Strauss, and R. G. Snyder*

Department of Chemistry, University of California, Berkeley, California 94720.
Received March 17, 1987

ABSTRACT: Glassy films of n-$C_{21}H_{44}$, n-$C_{36}H_{74}$, and low molecular weight polyethylene were prepared by vacuum sublimation onto a CsI window held at 7 K and were studied by infrared spectroscopy. The conformational disorder achieved for the glass was comparable to that of the liquid near the sublimation temperature. The chain-organizing processes were monitored for C_{21} and polyethylene as the sample was warmed to 300 K. A number of separate steps are involved. Each step occurs over a more or less broad temperature region, and sometimes the steps overlap. In the case of C_{21}, the first step involves a conformational ordering of the chains to their extended all-trans form. The extended chains initially pack in a monoclinic subcell, but they are not in longitudinal register; that is, the end methyl groups do not lie in parallel planes. At a higher temperature, the monoclinic subcell is converted to an orthorhombic subcell, but the chains are still not in register. In the last annealing step, which occurs over a narrow temperature range, the chains come into register so that the C_{21} finally assumes its stable orthorhombic crystal structure. The annealing of the polyethylene glass proceeds in exactly the same way except that there is no chain-registering step. In general, the transition temperatures are higher and the temperature range over which the transitions occur is broader for the polyethylene sample.

I. Introduction

There has accumulated over the years enormous literature on the polymethylene chain and its derivatives. There is good reason for this since this chain is an important and ubiquitous component of many natural substances and is a prototype synthetic polymer. Moreover, the polymethylene chain plays a unique role in model systems against which are tested new experimental and theoretical developments aimed at understanding the structure and dynamics of chain–molecule assemblies. It is then perhaps surprising to find that the glassy state of polymethylene systems has been studied so little. This is

† Present address: Groupe PCS, University of Geneva, 1211 Geneva 4, Switzerland.

0024-9297/87/2220-2810$01.50/0